NEW SEISMIC IMAGING OF THE COSO GEOTHERMAL FIELD, EASTERN CALIFORNIA

Jeffrey Unruh
William Lettis & Associates, Inc., 1777 Botelho Drive, Suite 262, Walnut Creek, CA 94598

Satish Pullammanappallil and William Honjas
Optim LLC, University of Nevada, Reno 89557

Francis Monastero
Geothermal Program Office, China Lake NAWC, CA 93555

ABSTRACT

New multifold seismic reflection data from the central Coso Range, eastern California, image brittle faults and other structures in Mesozoic crystalline rocks that host a producing geothermal field. The reflection data were processed in two steps that incorporate new seismic imaging methods: (1) P-wave first arrivals in the seismic data were inverted for subsurface acoustic velocities using a non-linear simulated annealing approach; and (2) 2-D Velocity tomograms obtained from the inversions were employed in pre-stack Kirchhoff migration to produce accurate, depth-migrated images of subsurface structure. Three-dimensional visualizations of the velocity structure show that discrete low velocity zones are associated with the two major producing areas of the Coso field, and that the producing zones are separated by a "ridge" of relatively higher velocity rock. The low velocity zones are interpreted to be zones of pervasive fracturing and/or hydrothermal alteration associated with localized hydrothermal circulation. The presence of the intervening "ridge" of high velocity rock, which presumably is relatively intact and unaltered bedrock, may indicate long-term compartmentalization of flow in the field. Kirchhoff depth-migrated seismic images reveal substantial coherent reflectivity in the upper 6 to 8 km of the crust. The Coso Wash fault, a Quaternary-active fault that is a locus of surface geothermal activity, is well-imaged as a moderately dipping reflector that terminates against a reflector or reflective zone at approximately 4 km depth. The 4 km reflective zone can be traced laterally beneath the geothermal field, and it may represent the brittle-ductile transition. The Kirchhoff images also reveal a prominent high-amplitude reflector at 6 km depth directly beneath the geothermal field. The reflector exhibits slight antiformal geometry and appears to be restricted to the northern part of the producing zone. The 6 km reflector tentatively is interpreted to be a pocket of magmatic brine or partial melt.

INTRODUCTION

This paper presents new seismic images of the Coso geothermal field in eastern California (Fig. 1). A total of 45 line-km of 2-D reflection data were acquired in the central Coso Range to test the ability of new processing methods to image structure in the crystalline rocks that host the geothermal field (Fig. 2). The data were processed using a combination of detailed velocity modeling and Kirchhoff pre-stack migration to obtain accurate, depth-migrated images

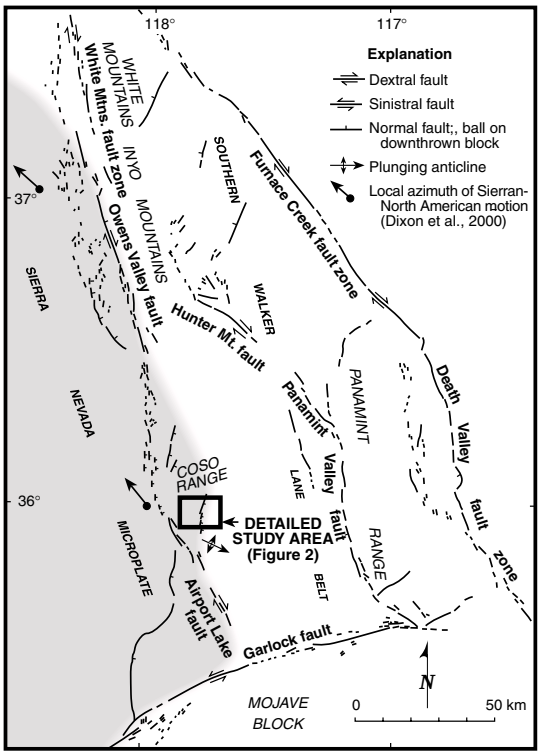

Figure 1: Major Quaternary faults of the southern Walker Lane belt (modified from Jennings, 1994). The shaded region depicts the Sierra Nevada microplate as defined by patterns of Quaternary faulting and geodesy (Dixon et al., 1995; King et al., 1999). Transfer of right-lateral shear across the right step between the Airport Lake fault and the Owens Valley fault drives localized crustal extension in the central Coso Range.

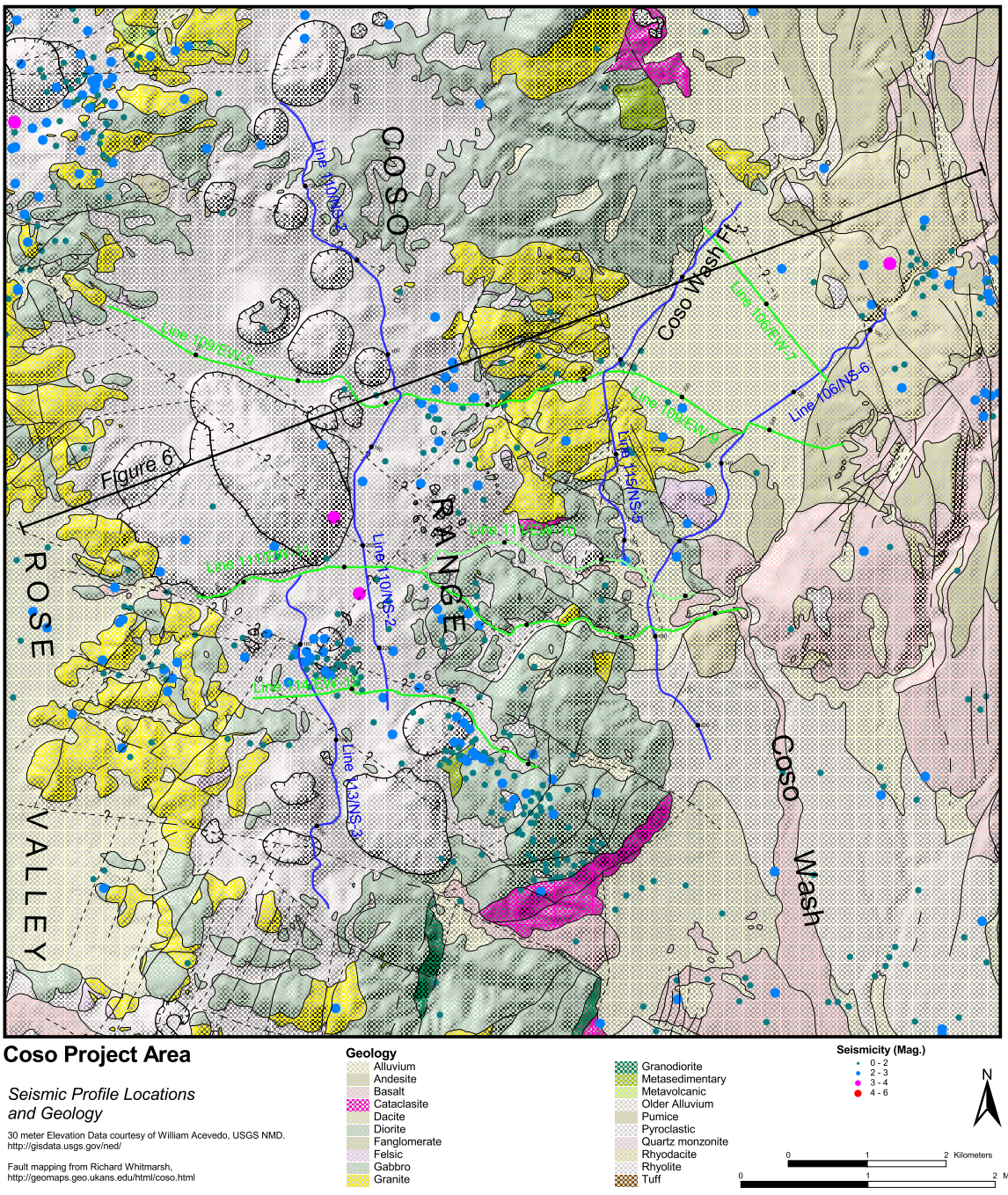

Figure 2: Geologic map of the central Coso Range showing locations of 2-D seismic reflection profiles acquired and processed for this study. Map data from R. Whitmarsh (Ph.D. dissertation, in progress).

of the subsurface structure (Pullammanappallil et al., 2001, this volume). A specific goal of this study was to image moderately to steeply dipping brittle faults and fractures that may control permeability and localize production in the field. The reflection data also were acquired to image deeper structures and assess their relationship to shallow faults that accommodate active strike-slip faulting and extension in the central Coso Range.

TECTONIC SETTING OF THE CENTRAL COSO RANGE

The Coso Range is a tectonically and volcanically active region along the eastern margin of the Sierra Nevada microplate, which moves about 13 mm/yr northwest with respect to stable North America (Argus and Gordon 1991; Dixon et al. 2000). Northwest motion of the Sierran microplate primarily is accommodated by distributed strike-slip and normal faulting in the Walker Lane belt, a 100-km-wide zone of active deformation bordering the eastern Sierra Nevada (Dixon et al., 1995; 2000). At a regional scale, crustal extension in the Coso Range is driven by a releasing stepover between the Airport Lake fault and the Owens Valley fault, two major right-lateral strike-slip faults (Fig. 1). Extension in the stepover region is accommodated in part by opening of Coso Wash, an asymmetric half graben that is bounded on the west by the Coso Wash fault. Hot springs, fumaroles and localized hydrothermal alteration are associated with the Coso Wash fault along the northeastern margin of the Coso geothermal field (Roquemore, 1980).

DATA ACQUISITION AND PROCESSING

Mesozoic intrusive rocks of the Sierra Nevada batholith underlie the Coso Range and host the Coso geothermal field (Duffield and Bacon, 1981). Layered reflective structure is absent or poorly expressed in such rocks, which traditionally have been regarded as "acoustically transparent" for the purposes of seismic reflection imaging. This study uses a new processing approach to improve imaging of moderately to steeply dipping faults and fractures associated with lateral velocity contrasts in crystalline rocks. The processing consists of the following steps:

1) P-wave first arrivals in the seismic data for individual lines are inverted to obtain the shallow 2-D velocity structure (i.e., a velocity tomogram) along the line. The inversion is performed using a proprietary software called SeisOpt @2D (© Optim LLC 2000).

2) Kirchhoff pre-stack seismic images are developed for each line by using the velocity tomograms as a basis for migrating the reflection data. Pre-processing of the data (muting, filtering, etc) was performed prior to the migration.

A more detailed description of the data acquisition parameters and processing approach is presented in Pullammanappallil et al. (this volume).

RESULTS

Correlation of Shallow Velocity Structure to Producing Zones in the Coso Field

We interpolated the shallow velocity structure between individual 2-D seismic lines to develop a 3-D model of lateral velocity variations beneath the geothermal field. A commercial software (SlicerDicer, ver. 3.0.3, (c) copyright 1988-2000 Pixotec LLC) was used for 3-D visualization of the 2-D data.

Individual 2-D velocity tomograms show that a low velocity zone is present in the 1.0 to 1.5 km depth range beneath the main production area of the Coso field, and beneath a producing area known as the "East Flank" (Fig. 3). The average velocity of these zones is about 4.6 km/s (15,000 ft/s), compared to

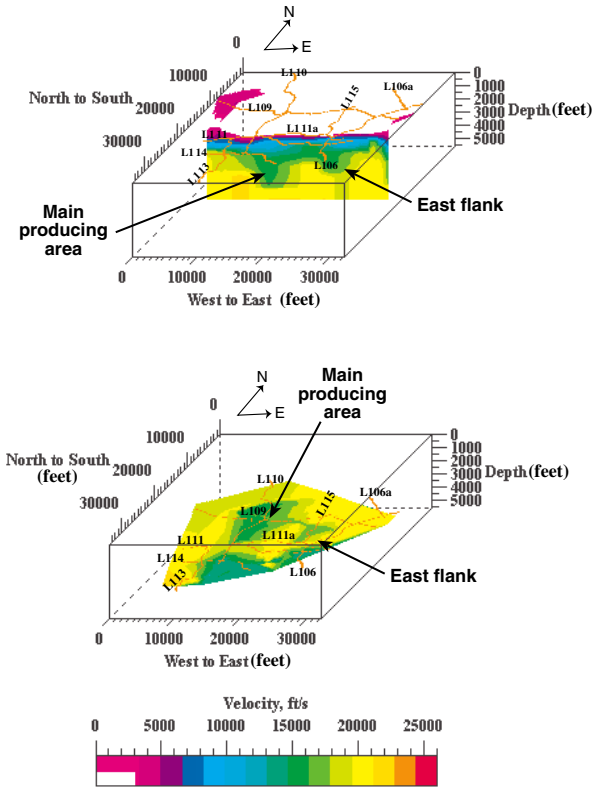

Figure 3: Selected views through the 3-D velocity model of the central Coso Range showing low velocity zones associated with the main producing area and East Flank production zones.

crystalline bedrock velocities of about 6.1 km/s (20,000 ft/s) outside the zones. The low velocity zones also are associated with an aeromagnetic low intensity anomaly that is centered on the producing area (Plouff and Isherwood, 1980). The 3-D velocity model helps delineate the extent and geometry of the two low velocity zones, and it reveals a north-south-trending "ridge" of high velocity rocks separating them (Fig. 3).

We tentatively attribute the reduced acoustic velocity of the producing zones to pervasive fracturing and/or hydrothermal alteration of the crystalline rocks. Extensive alteration could destroy primary magnetite in the bedrock and thus account for the magnetic low over the geothermal field. If this interpretation is correct, then the high velocity "ridge" between the two low velocity zones may be relatively unaltered bedrock, indicating long-term compartmentalization of hydrothermal circulation in the two main producing areas.

Reflection Imaging

Imaging Brittle Faults

A major objective of this study is to test the ability of the data acquisition and processing approach to image brittle faults and other potentially permeable features in crystalline rocks. To this end, multiple seismic lines were acquired across northern Coso Wash graben (Fig. 2). Of particular interest is the down-dip geometry of the Coso Wash fault, which is associated with hot springs, zones of alteration and other surface manifestations of hydrothermal activity.

The Coso Wash fault is clearly imaged as a moderately east-dipping reflector in the processed data (Fig. 4). West-dipping reflectors in the hanging wall of the Coso Wash fault are correlated with antithetic faults exposed along the eastern margin of the graben (Fig. 2 and 4). The Coso Wash fault flattens abruptly or soles into a faint but discernable reflecting horizon at about 4 km depth that can be traced laterally beneath Coso Wash, and westward beneath the geothermal field.

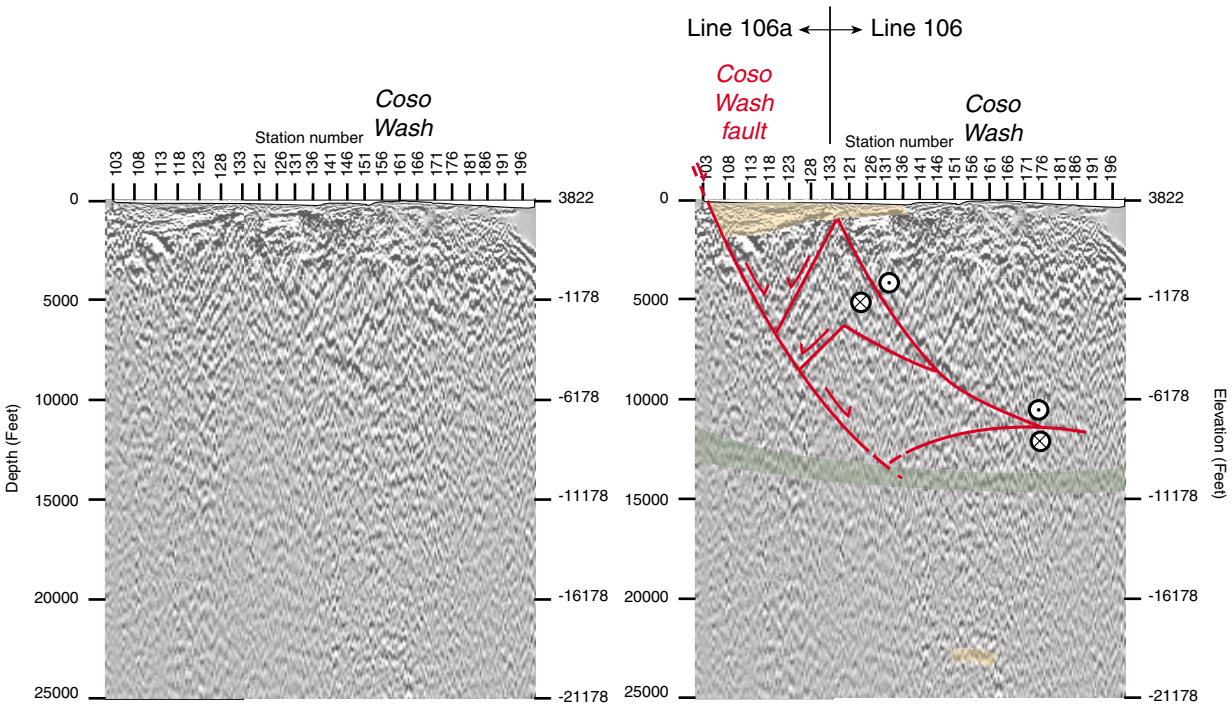

Figure 4: Composite north-south depth-migrated seismic line through Coso Wash formed by joining lines 106 and 106a (see Fig. 2 for locations of seismic lines). The crossing geometry of lines 106 and 106a provides three dimensional views of the antithetic faults and their termination against the Coso Wash fault. Note discontinuous deep reflectors in the 6-7 km depth range (20,000-23,000 ft).

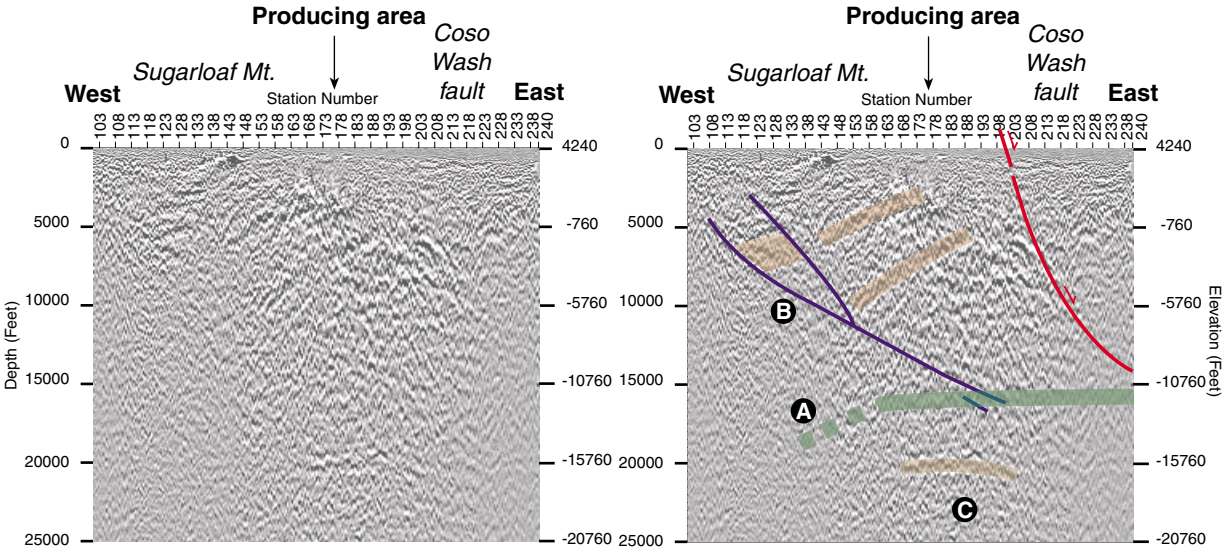

Figure 5: East-west depth-migrated line 109 passes through the main producing areas of the Coso field (see Fig. 2 for location of line). The surface trace of the Coso Wash fault is correlated with an east-dipping reflector that can be traced down-dip to a depth of about 4.3 km (14,000 ft), where it appears to terminate against or merge with the subhorizontal reflective zone (A) imaged on lines 106 and 106a (Fig. 4). Moderately east-dipping reflectors west of the Coso Wash fault (B) also appear to terminate against the 4 km reflecting horizon. West-dipping reflectors appear to terminate against the B reflectors. A high amplitude reflector (C) present at 6 km depth (20,000 ft) beneath the geothermal field is associated with a zone of reflectivity or discontinuous reflectors that can be traced laterally beneath most of the seismic reflection array.

Deep Reflectors

The depth-migrated data consistently image a 1- to 2-km-wide zone of discontinuous reflectors in the 6-9 km depth range beneath the seismic array (Fig. 4). The reflectors can be traced laterally and clearly correlated on crossing lines, and thus do not appear to be processing artifacts.

A striking high-amplitude reflector is present within this zone at 6 km depth beneath the main production area (Fig. 5). This feature is located beneath and adjacent to some of the youngest volcanic features in the central Coso Range (Duffield and Bacon, 1981). The reflector is coincident with a low-velocity teleseismic S-wave converter at 6 km depth observed via receiver function studies (C.H. Jones, personal communication, 2000). We interpret the high amplitude reflector to be a localized zone of fluids and/or partial melt.

TECTONIC INTERPRETATION

The Coso geothermal field is associated with a zone of localized crustal extension in a releasing stepover between two major strike-slip faults. Extension of the upper 4 km of the crust is accommodated by brittle faulting within the field and opening of the Coso Wash graben to the east (Fig. 6). The brittle faults appear to sole into or terminate against a subhorizontal reflecting horizon at 4-5 km depth; we tentatively interpret this horizon to be the brittle-ductile transition, consistent with the observation that most seismicity in the vicinity of the geothermal field and western Coso Wash graben is confined to the upper 4 to 5 km (Fig. 6). Ductile stretching of the crust and emplacement of shallow igneous bodies may accommodate extension at depth, and particularly beneath the geothermal field. The high amplitude reflector at 6 km depth beneath the geothermal field may be a magmatic sill or a zone of fluid derived from a magma body below 6 km. The intrusions provide a localized source of heat that confines brittle deformation to the upper 4-5 km of the crust and drives hydrothermal circulation in the field.

DISCUSSION

The structure beneath the Coso field in Fig. 6 is similar to a generalized model proposed by Fournier (1999) for hydrothermal processes in magmatic-epithermal environments. In Fournier's model,

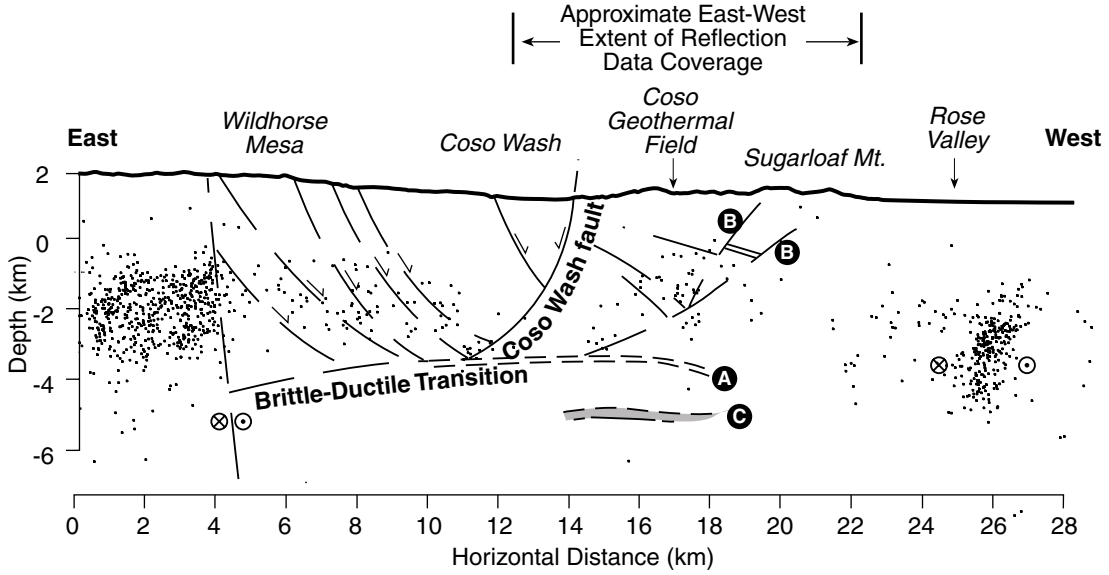

Figure 6: Interpreted relationship between major features imaged on lines 106 and 109, mapped geology and seismicity (events recorded by the Southern California Seismic Network). Reflector A lies at or near the base of seismicity and is interpreted to be the local brittle-ductile transition zone beneath the Coso field. Brittle faulting accommodated by the southeast-dipping Coso Wash fault and antithetic faults of Wildhorse Mesa is confined to the upper 4 km above the brittle-ductile transition. East-dipping reflectors west of the Coso Wash fault (B) underlie Sugarloaf Mt. and some of the youngest volcanic domes in the Coso Range. These reflectors may be moderate to low-angle normal faults or magma conduits. The high-amplitude reflector at 6 km depth beneath the geothermal field (C) is interpreted to be a lens of fluid or a magmatic sill.

emplacement of a magma body may locally elevate the brittle-ductile transition zone to shallow depths. The transition zone separates a hydrostatically pressured domain above, in which meteoric water flows convectively, from a lithostatically pressured domain below. Depending on the orientations and relative magnitudes of the principal stresses, fluids expelled from underlying magma bodies may accumulate in horizontal lens-like bodies below the brittle-ductile transition zone. According to Fournier (1999), the self-sealed transition zone may periodically be breached by brittle failure, allowing trapped hypersaline brine and gas to be expelled upward into the brittle domain.

SUMMARY AND CONCLUSIONS

New processing approaches used for this study demonstrate that seismic imaging can provide valuable information about the structure of a geothermal field hosted in crystalline (i.e., 'transparent") rocks. Data on the shallow velocity structure from inversion of P-wave first arrival times in the seismic data reveal that producing areas of the Coso field are associated with relatively lower acoustic velocities, which we attribute to localized brittle faulting and hydrothermal alteration. If this interpretation is correct, and if it can be generalized to other geothermal regions, then it suggests that velocity models obtained in the course of processing reflection data may be a useful geothermal exploration tool. Depth-migrated images that incorporate detailed velocity data reveal substantial reflective structure in the upper 6-8 km of the crust, including brittle faults and deeper features that are possibly related to magmatic activity. These data provide new insights into active tectonic and magmatic processes in the central Coso Range.

REFERENCES

Argus, D.F., and Gordon, R.G. (1991), "Current Sierra Nevada-North America motion from Very Long baseline interferometry: implications for the kinematics of the western United States", *Geology*, **19**, 1085-1088.

Dixon, T.H., Robaudo, J.L., and Reheis, M.C. (1995), "Constraints on present-day Basin and Range deformation from space geodesy", *Tectonics*,**14**, 755-772.

Dixon, T.H., Miller, M., Farina, F., Wang, H., Johnson, D. (2000), "Present-day motion of the

Sierra Nevada block and some tectonic implications for the Basin and Range province, North American Cordillera", *Tectonics*, **19**, 1-24.

Duffield, W.A., and Bacon, C.R. (1981), "Geologic map of the Coso Volcanic field and adjacent areas, Inyo County, California", *U.S. Geological Survey Miscellaneous Investigations Series*, **Map I-1200**, scale 1:50,000.

Fournier, R. (1999), "Hydrothermal processes related to movement of fluid from plastic into brittle rock in the magmatic-epithermal environment", *Economic Geology*, **94**, 1193-1212.

Jennings, C.W. (1994), "Fault activity map of California and adjacent areas", *California Department of Conservation, Division of Mines and Geology*, **Geologic Data Map No. 6**, scale 1:750,000.

King, R.W., Hager, B.H., McCluskey, S.C., and Meade, B.J. (1999), "Reduction and utilization of GPS data from the Navy geothermal crustal motion network", *Final Technical Report prepared for the Geothermal Program Office, Naval Air Warfare Center, China Lake, CA*, Contract No. N68936-95-C-0371, 30 p.

Plouff, D., and Isherwood, W.F. (1980), "Aeromagnetic and gravity surveys in the Coso Range, California", *Journal of Geophysical Research*, **85**, 2491-2501.

Pullammanappallil, S., Hanjas, W., Unruh, J., and Monastero, F. (2001), "Use of advanced data processing techniques in the imaging of the Coso geothermal field", this volume.

Roquemore, G. (1980), "Structure, tectonics and stress field of the Coso Range, Inyo County, California", *Journal of Geophysical Research*, **85**, 2434-2440.